Bollettino di Geofisica Teorica ed Applicata Vol. 52, n. 4, pp. 707-728; December 2011
DOI 10.4430/bgta0022

Differentiation between boulders deposited by tsunamis and storm waves along the south-eastern Ionian coast of Sicily (Italy)

M.S. Barbano, F. Gerardi and C. Pirrotta

Dipartimento di Scienze Geologiche, Università di Catania, Italy

(Received: April 2, 2010; accepted: September 24, 2010)

ABSTRACT Boulders in three areas (Capo Campolato, Vendicari, and San Lorenzo) along the Ionian coast of Sicily were analyzed, in order to distinguish if they were deposited by storm waves or tsunamis. On the whole, the size, shape, position and long-axis orientation of 328 boulders were accurately evaluated. These mega-clasts were deposited from the sea or moved from the gently sloping rocky coast and distributed within 80 m from the shoreline. Most boulders are rectangular, with sharp, broken edges. They are calcarenite fragments, estimated up to 71 t in mass. Some of the boulders (up to 32 m from shore and up to about 6 t) were observed to have moved after strong winter storms occurred from December 2008 to January 2009, whereas the positions of many other boulders were unchanged. We used hydrodynamic equations jointly with statistical analysis of boulders in order to determine the extreme events (geological or meteorological) responsible for these singular accumulations. Using the wave height and period of maximum observed storms and of historical tsunamis (1693 and 1908 events) along the Ionian coast of Sicily, we estimated the approximate transport distance at which the waves are capable of depositing boulders inland. Results show that the largest storm waves were probably responsible for the current distribution of most boulders, whereas the boulders at a distance > 40 m are likely deposited by tsunamis.

Key words: boulders, tsunami, Sicily.

1. Introduction

Boulder deposits along the coast can represent markers of important geological or meteorological phenomena since their emplacement is usually attributed to the impact of high-energy waves (tsunamis, hurricanes or powerful storms) on the rocky coast. These accumulations have recently been analyzed in different tectonic and geomorphological contexts to distinguish the mechanism responsible for their emplacement. They appear as isolated mega-boulders [e.g., up to 1500 t in French Polynesia and in the Bahamas: Bourrouilh-Le Jan and Talandier (1985); Kelletat *et al*. (2004)] or fields of scattered boulders up to hundreds of meters inland on coastal platforms (e.g., Mastronuzzi and Sansò, 2000; Noormets *et al*., 2002; Whelan and Kelletat, 2005; Scheffers and Scheffers, 2007; Paris *et al*., 2009), cliff-top boulders (e.g., De Lange *et al*., 2006; Hall *et al*., 2006; Etienne and Paris, 2010), boulder ridges and ramparts (Scheffers, 2004; Mastronuzzi *et al*., 2007).

Differentiating the boulder transport mechanism, whether by tsunami or storm waves, is a topic of growing interest in the literature (e.g., Nanayama *et al*., 2000; Goff *et al*., 2004; Kortekaas and Dawson, 2007; Morton *et al*., 2007; Goto *et al*., 2010). Nevertheless, few documented examples exist of boulders clearly displaced by historical tsunamis (e.g., Goff *et al*., 2006; Goto *et al*., 2007, 2009; Paris *et al*., 2009; Bourgeois and MacInnes; 2010) and by storm waves (e.g., Mastronuzzi and Sansò, 2004; Scheffers and Scheffers, 2006; Goto *et al*., 2009; Hansom and Hall, 2009; Barbano *et al*., 2010). Hence, no definitive criteria have been advanced to discriminate between tsunami and storm wave boulders (e.g., Dawson *et al*., 2008; Kelletat, 2008). Distinguishing boulders deposited by tsunamis from those deposited by storms and determining the age of their deposition can help to evaluate the magnitude and frequency of tsunamis along coastal areas and therefore to assess coastal hazards.

Along the coasts of the Mediterranean Sea, several authors have discussed the origin of boulder fields: boulder accumulation on the Algerian coast was interpreted as evidence of tsunamis occurring in the western Mediterranean (Maouche *et al*., 2009); large volumes of coarse rocky material, including boulders weighing over 20 t, were interpreted as having been shifted by tsunamis taking place on Cyprus during the last few centuries (Kelletat and Schellmann, 2002). Mastronuzzi and Sansò (2000, 2004) attributed calcarenitic megaclasts of Pleistocene age (up to 80 t), scattered along the Ionian coast of Apulia (Italy), to three tsunami events between the 15th and 18th centuries AD. In south-eastern Sicily, anomalous deposits of calcarenitic boulders were studied by Scicchitano *et al*. (2007). The authors analyzed boulders, scattered along wide terraces 2-5 m a.p.s.l. (above present sea level), in four distinct sites between the towns of Augusta and Siracusa and concluded that these accumulations were detached and transported by historical tsunamis. Recently, Barbano *et al*. (2010), analyzing a boulder accumulation at Vendicari (the southernmost tip of eastern Sicily), showed that the largest storms seem to be responsible for their deposition; only some boulders are likely deposited by tsunamis considering their size and distance from the shoreline.

In this paper, we study boulder accumulations in two additional areas along the south-eastern Ionian coast of Sicily, namely Capo Campolato and San Lorenzo, and compare them with the results of Barbano *et al*. (2010). To this end, we conducted a morphological analysis of the shore and performed field surveys at different times (before and after winter storms), mapping the boulders and describing in detail their setting, sizes, shape, their probably pre-transport position, arrangement (if single block or packed) and distance from the shoreline. Moreover, we analyzed the storm-wave regime of the Ionian coast of Sicily and estimated the storm wave heights and their maximum flooding at the study areas. Therefore, we compared the ondametric data with the boulder setting to assess the minimum wave height required to emplace the boulders in their inland position and the transport limit distance of known storm waves and historical tsunamis.

2. Tsunami or storm boulders: previous approaches

With the aim of distinguishing boulders deposited by tsunamis from those deposited by storms, several models have been proposed in literature, generally combining field observations with hydrodynamic equations.

Nott (1997, 2003) proposed hydrodynamic equations to estimate the wave height necessary to

start the boulder movement, on the basis of their pre-transport setting. Although this method is often used worldwide for testing the origin of the boulders (e.g., Scheffers and Kelletat, 2006; Bryant and Haslett, 2007; Mastronuzzi *et al*., 2007; Scheffers *et al*., 2008), several authors have pointed out that the model incorporates some assumptions without sufficient evaluation of their applicability and that wave heights calculated by Nott's (2003) equations appear misestimated (e.g., Morton *et al*., 2006, 2008; Kelletat, 2008; Goto *et al*., 2009; Paris *et al*., 2010; Switzer and Burston, 2010).

Hydrodynamics of boulder detachment and transport on a shore platform have been dealt with by Noormets *et al*. (2004) who also introduced the wave period in the transport mechanism on the shore platform and linked the wave height at the breaking point to the inland wave flooding. Indeed, according to Noormets *et al*. (2004), both the wave height and the wave period influence the attenuation velocity and thus the limit of flooding on the coast and its ability to transport boulders inland. These parameters differ between storm waves and tsunamis, the latter are characterized by considerably longer periods than storm waves. Noormets *et al*. (2004) noted that shorter, ca. $T = 8$ s, waves have greater quarrying capacity due to the higher pressure exerted on the face of the cliff as compared to those of longer waves, whereas the transporting capacity of waves augments with increasing wave length. Therefore, the significant parameter that distinguishes boulders deposited by storm waves from those deposited by a tsunami could be their distance from the coastline.

Imamura *et al*. (2008) studied various mechanisms of boulder transport, i.e., sliding, rolling, and jumping, and estimated tsunami hydraulic values, but they did not model the storm scenario. Hansom *et al*. (2008) investigated the processes of cliff-top erosion and deposition under extreme storm waves, showing that they are capable of quarrying, transporting and depositing large blocks at significant altitude and distances inland and so present serious questions about the use of such deposits as indicative of tsunamis.

Pignatelli *et al*. (2009) estimated the wave heights necessary to move boulders thus slightly modifying Nott's (2003) equations and, considering local morphological features and coast roughness, evaluated the maximum tsunami inundation using the equations proposed by Hills and Mader (1997) but they did not assess storm flooding on the coast.

Numerous and complex processes in boulder deposition co-occur. Local variation of topography, roughness of the rocky coast, initial setting and possible backwash transport of the boulders should be considered but such complexities are difficult to incorporate into simple hydrodynamic models (Goto *et al*., 2010). So in this paper, we hypothesized that boulders are moved by only a wave and that no backwash flow occurred and we used the hydrodynamic equations proposed by Noormets *et al*. (2004) in order to verify the boulder displacement cause. Indeed, the emplacement distance depends on the capacity of a wave to attenuate when it moves inland and this characteristic is linked to both breaking wave height and wave period that differs between storm and tsunami waves. Nott's (2003) approach, often adopted to discriminate tsunami and storm boulders, does not consider their final position on land.

3. The study areas

3.1. Geological setting and historical tsunamis

The study areas are located on the southern Ionian coast of Sicily, that represents the emerged

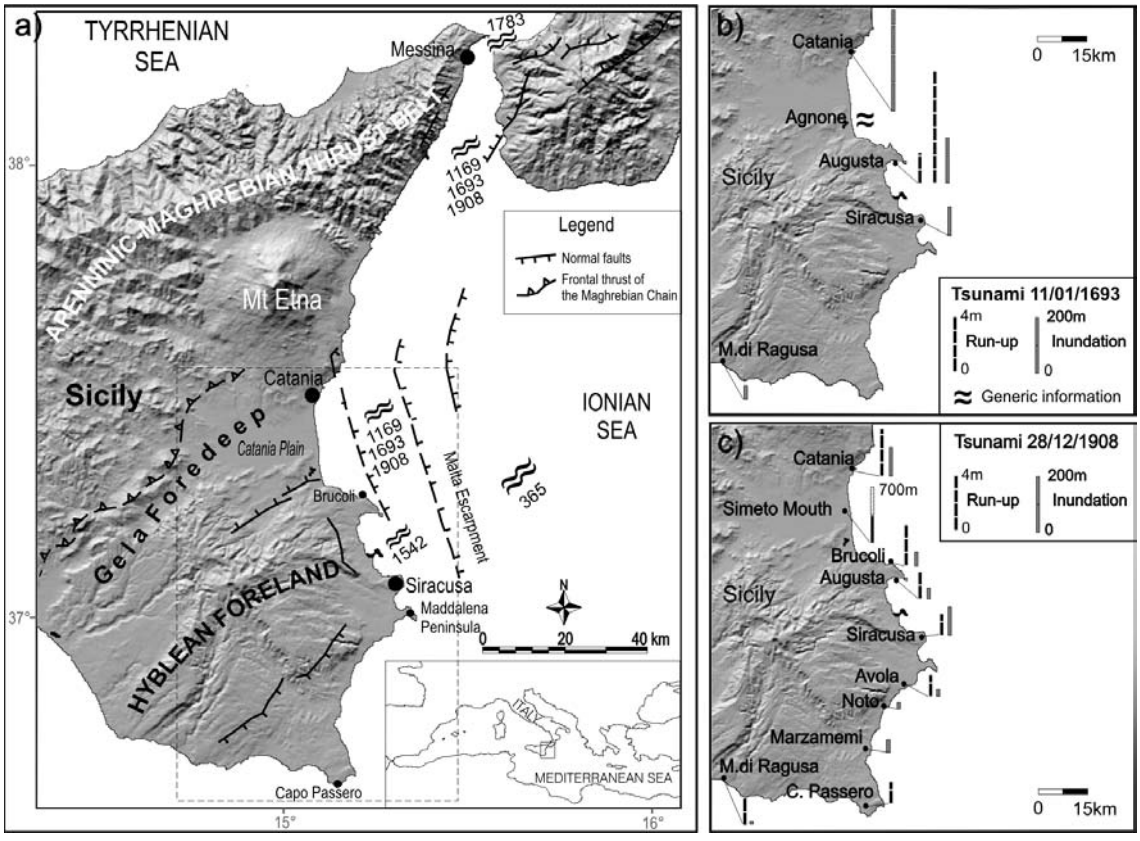

Fig. 1 - a) Map of eastern Sicily showing the main structural domains, seismotectonic features, date of the main historical tsunamis affecting the eastern coast of Sicily and inundated areas; b) and c) detailed run-up and inundation data for the 1693 and 1908 tsunamis, respectively, in south-eastern Sicily (from Gerardi *et al*., 2008).

eastern part of the Hyblean foreland domain of the Apenninic Maghrebian Chain (Lentini *et al*., 1994). Normal fault systems in eastern Sicily, mostly located offshore, control the Ionian coast from Messina to the eastern flank of Mt. Etna, joining up southwards with the fault system of the Malta Escarpment (Fig. 1). These faults were probably responsible for historical earthquakes with M_w up to 7.4, such as the 1169, 1693 and 1908 events (Working group CPTI, 2004), that generated devastating local tsunamis (Tinti *et al*., 2007). The Sicilian Ionian coast also experienced the effects of tsunamis originating from distant sources, such as those belonging to the Aegean zone [e.g., the A.D. 365 Crete earthquake: Guidoboni *et al*. (1994), Tinti *et al.* (2005), Lorito *et al*. (2008)] (Fig. 1). During the last 2000 years, the 250-km long Ionian coast of Sicily has been affected by at least 11 historical tsunamis (Tinti *et al*., 2007) and geological evidence of several paleoinundations has also been found (Barbano *et al*., 2009; De Martini *et al*., 2010). Nevertheless, detailed historical information about tsunami parameters in south-eastern Sicily concerns only the 1693 and 1908 events (Figs. 1b and 1c), for which historical accounts reported run-up and inundation values (Gerardi *et al*., 2008).

The south-eastern edge of the Hyblean plateau is characterized by a rocky coast that, from Brucoli to Capo Passero shows a flat landscape, weakly incised by a poorly developed

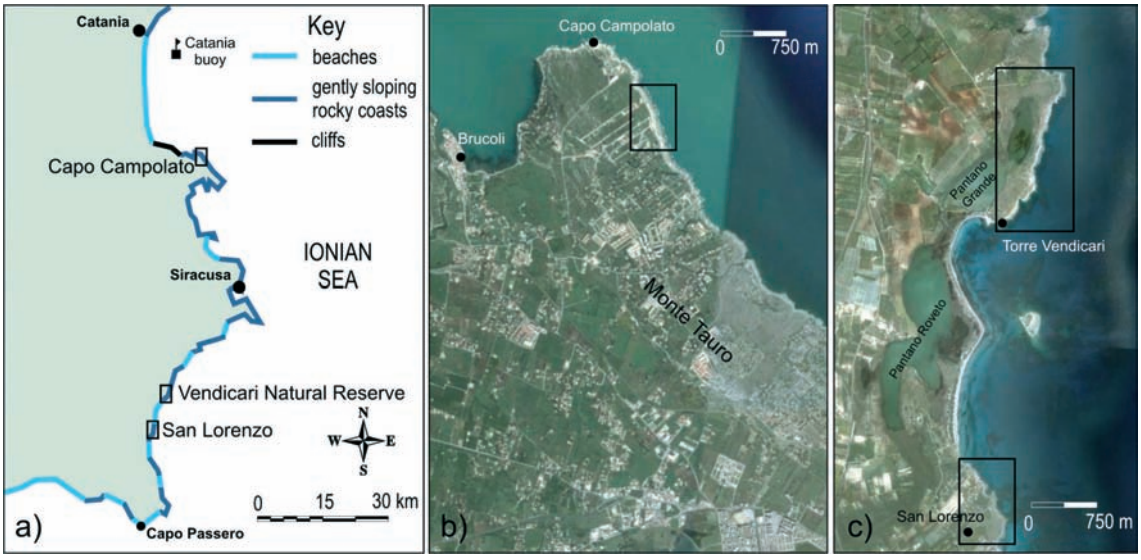

Fig. 2 - a) Eastern Sicily morphological coastal types from Catania to Capo Passero. Black rectangles show the study areas. b) Monte Tauro Peninsula Google Earth map, black rectangle shows the Capo Campolato area (detail in Fig. 3); c) Google Earth map of the southern study area, black rectangles show, in the northern part, the Vendicari Nature Reserve area, studied by Barbano *et al*. (2010), and in the southern part the San Lorenzo area (detail in Fig. 4).

hydrographic network and in some areas rises to form high cliffs (Fig. 2a). We focused our study on Capo Campolato (Fig. 2b), located in the northern tip of the Mt. Tauro Peninsula, and the San Lorenzo site (Fig. 2c), located south of the Vendicari Nature Reserve.

3.2. Wave climate framework

The Mediterranean basin is characterised by a highly indented coastline that creates some small and well-defined sub-basins. Here, the wave energy is conditioned by wind speed and by limited fetches (Lionello *et al*., 2006). Hurricanes are absent in the Mediterranean basin, although tropical-like cyclones (Emanuel, 2005) have been identified in the past and their dynamics studied (e.g., Pytharoulis *et al*., 2000; Gianfreda *et al*., 2005; Monserrat *et al*., 2006; Fita *et al*., 2007).

In order to assess the storm-wave regime on the Ionian coast of Sicily and to estimate the storm wave heights at the study areas, we analyzed the anemometric and ondametric data, recorded by the nearest meteo-marine Catania station belonging to the RON - Rete Ondametrica Nazionale (= Italian Sea Wave Network, www.idromare.it) for the available period 1989–2006 (APAT, 2006). The analysis of waves with maximum height $H > 3$ m at the Catania buoy showed that the Ionian Sea is exposed to wind-generated storms coming prevalently from eastern and south-eastern directions, and the strongest events, usually occurring between November and March, with $H > 5.5$ m, are confined to the range N90°E - N110°E. The Catania buoy recorded a maximum offshore wave height of 6.2 m in February 1996 from E-SE with a peak period of 11.1 s, a wave with maximum peak period of 28.6 s and height of 4.1 m from NE in October 2004 and a wave with maximum peak period of 28.6 s and height of 3.35 m from SE in January 2005

Table 1 - Storm events with maximum wave height (H_0) and peak period (T_0) in deep water recorded by the Catania buoy, used for Capo Campolato, and transposed for Vendicari and San Lorenzo site (H_T and T_T).

Date	Wave data from Catania bouy			Wave data in Capo Campolato site				Wave transposed data			Wave data in Vendicari site			Wave data in San Lorenzo site		
	Direction (N)	H_0	T_0	L_0(m)	β_1(°)	CWH_b (m)	CX_{max} (m)	H_T	T_T	L_0 (m)	β_2(°)	VWH_b (m)	VX_{max} (m)	β_3(°)	SWH_b (m)	SX_{max} (m)
31/03/1991	70°	5.1	9.1	129.3	5.0	7.0	14.5	5.6	9.7	147.6	2.0	6.5	14	1.2	5.8	13.2
26/12/1992	94°	5.8	11.1	192.4		8.5	18.8	6.1	11.4	204.8		7.5	18		6.7	16.7
28/02/1996	104°	6.2	11.1	192.4		8.9	19.2	6.4	11.4	201.6		7.8	18		6.9	16.8
17/03/2003	162°	3.8	13.3	276.3		6.8	23.7	5.1	16.1	404.4		7.7	25		6.9	23.8
04/10/2004	40°	4.1	28.6	1277.7		10.6	57.6	4.5	31.4	1546.1		9.9	58		8.9	52.8
05/01/2005	129°	3.0	28.6	1277.7		8.4	49.8	3.3	30.5	1454.1		7.8	48		6.9	43.3
12/01/2005	119°	3.3	28.6	1277.7		9.1	50.5	3.6	29.7	1383.5		8.1	48		7.2	45

β_1, β_2 and β_3 are the average sea bottom slope from –20 m depth to the shoreline at Capo Campolato, Vendicari and San Lorenzo, respectively, as measured from the nautical maps of the Italian Marine Hydrographic Institute (Istituto Idrografico della Marina, 1999) at scale 1:100,000. The estimated wave length in deep water [$L_0=gT^2/2\pi$; Sarpkaya and Isaacson, 1981)], and the wave height at breaking point at Capo Campolato (CWH_b), Vendicari (VWH_b) and San Lorenzo (SWH_b), are determined with the Sunamura and Horikawa (1974) equation ($Hb/H_0=(\tan\beta)^{0.2}(H_0/L_0)^{-0.25}$). CX_{max} = Capo Campolato; VX_{max} = Vendicari and SX_{max} = San Lorenzo are the maximum water flooding of the strongest storm waves in the study areas, obtained using the equations of Cox and Machemel (1986) and Noormets *et al.* (2004) (see chapter 5.2).

(Table 1). Even if the available ondametric data refer to a short time interval, they probably include storms with plausible maximum peak period and maximum wave height for the Ionian Sea, since some of the strongest storms occurring in the analyzed period have been classified as tropical-like cyclones (Pytharoulis *et al*., 2000). These buoy values seem to be compatible with the Ionian wave regime and, according to Pignatelli *et al*. (2009), different to that of the oceanic context, where waves reach greater heights and have shorter periods than those in the Mediterranean Sea.

The tides observed at the Catania meteo-marine station, range from +0.37 to -0.31 m (www.idromare.it), hence the coastal area of Sicily can be considered micro-tidal since the tide range does not exceed 0.60 m. Along the study area, we also observed a tide marker on a small cliff at San Lorenzo where a notch indicates a tide of about 30 cm.

The wave height and the peak period depend on the sector of maximum prevailing wind and efficacious fetch lengths. Capo Campolato is located about 20 km south of the Catania buoy (Fig. 2a) within its prevailing wind area and fetch length; so, we used the data registered by the Catania buoy to compute the maximum wave height at this site. Vendicari and San Lorenzo are placed about 70 km south of the Catania buoy, therefore, in order to compute wave height and period at these sites we used the transposition technique (Seymour, 1977) that allows us to determine calibration coefficients with respect to the reference site. To apply the transposition method, we estimated the sector of maximum prevailing wind and efficacious fetch lengths related to Vendicari and San Lorenzo. The prevailing wind sector in this area is confined to NNE in the direction of the Maddalena Peninsula and to SSE in the direction of Capo Passero (Fig. 1). We

computed the significant wave height H_T and the peak period T_T as a function of fetch length and wind velocity, applying Vincent's (1984) equation for Vendicari and San Lorenzo, using the RON Catania buoy data (Table 1). Given that the buoy data are in deep water, we estimated wave length in deep water (Sarpkaya and Isaacson, 1981) and then we obtained wave heights at breaking point at Capo Campolato (CWH_b), Vendicari (VWH_b) and San Lorenzo (SWH_b), using the Sunamura and Horikawa (1974) equation (Table 1).

4. Field observations

Since boulder movement by waves depends on a wide variety of parameters, we estimated boulder size, shape, pre-transport setting and arrangement (if single block or packed). Moreover, we made three different GPS surveys to obtain the position of each boulder with respect to the shoreline trend (Figs. 3a and 4a) and to measure eventual boulder displacement due to winter storms: the first survey during September 2006, the second during October 2008-February 2009 and the last one in January-March 2010.

We carried out direct observations on each boulder of its form and the erosion/encrustation markers. For each boulder, whose shape can generally be approximated to a parallelepiped, we measured the lengths of the three axes (A-axis > B-axis > C-axis), the longest axis orientation, the distance from the shoreline (m) and, lastly, we assessed the volume. Since the parallelepiped boulder shape is imperfect, we averaged three or more measurments along each axis. Attention was restricted to boulders with lengths of more than 1 m along the longest axis.

At Capo Campolato and San Lorenzo we analyzed 153 boulders in all (Figs. 3a and 4a), generally showing a rectangular shape, occasionally prismatic subangular, and sometimes with sharp broken edges (Figs. 3b and 4b). We collected rocky samples from the dislocated blocks for unit weight laboratory measurements. We also evaluated the probable environment and setting, preceding block transport, by considering the megaclast characteristics, e.g., if it is totally or partially encrusted, if bordered by fractures or if showing other littoral marine features.

4.1. Capo Campolato area

Capo Campolato is located in the northern tip of the Monte Tauro promontory, bounding the northern side of Augusta Bay. In this area, the calcirudite, with algae and bryozoa, and the white-yellowish calcarenites of the Monte Climiti Formation (middle Miocene) outcrop (Lentini *et al.*, 1994). Along the coast, this formation creates a gently sloping, rocky platform, oriented NNW-SSE and highly eroded by the karstification, with the development of wide littoral pools. Moreover, it is affected by a dense fracture network that facilitates the platform erosion and sometimes the development of long and depressed NNW-SSE trending areas. Locally, a red organic calcarenite fills the depressions on the platform. This transgressive deposit might represent the same marine formation, probably of Pleistocene age, observed in the southernmost Vendicari site (Lentini *et al.*, 1994). Since this formation is at about 1 m a.p.s.l., we can consider a very low uplift rate for the area since the Pleistocene age, also according to Antonioli *et al.* (2009), that estimated a Holocene uplift of 0.07 mm/y here.

The sector was investigated over a 750 m long area. The gently sloping, rocky coast has a

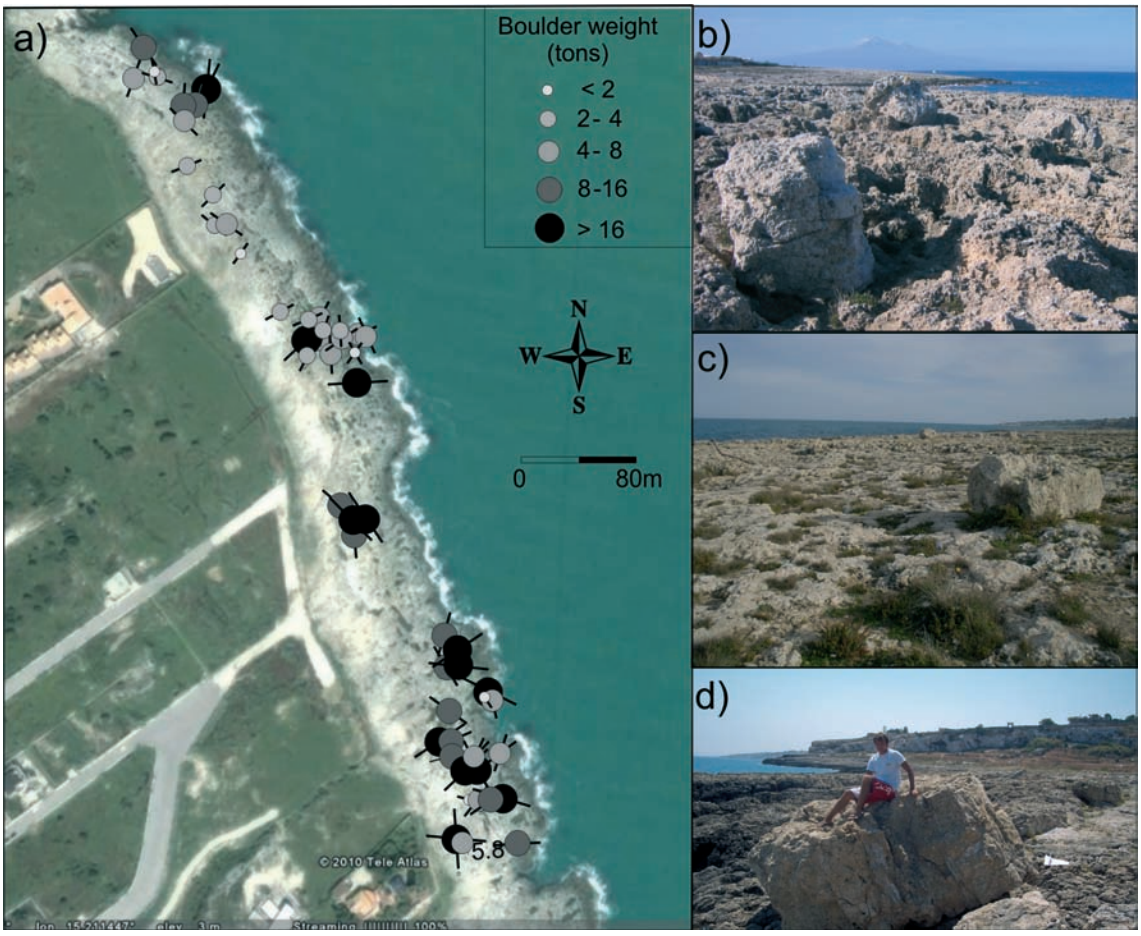

Fig. 3 - Google Earth map showing the boulder location along the Capo Campolato coastland (for location see Fig. 2) dots indicate the different boulder weighs and black lines indicate A-axis orientation (a); view of the boulder accumulation in: the northern area (b), the central area (c), and the southern area (d).

maximum width of about 80 m from the shoreline, reaching a maximum height of about 8-10 m a.p.s.l. with an average slope of 10°, beyond this distance the vegetated berm develops.

Sixty-three boulders, constituted by the carbonate rocks of Mt. Climiti Fm., were surveyed and studied in detail. These megaclasts are generally very big and far from the coastline, with a maximum distance of about 80 m (Fig. 3a). On average, the boulders have a volume of about 5.0 m^3 and an estimated weight of about 11 t (assuming an average density of 2.4 g/cm^3 based on laboratory analyses); the heaviest one is about 71 t at 10 m from the shoreline (Fig. 3d). The majority of the blocks lie at the limit of the vegetated berm, on a loose deposit, made of soil and rich in shell fragments from the sandy beach. Moreover, some boulders have plants on their surface (Fig. 3c).

These megaclasts have neither biogenic encrustations (e.g., vermetids, serpulids or algae) nor erosive littoral features (e.g., pools and potholes). Only some boulders show highly eroded and empty Lithophaga bores. Instead, they are characterized by a marked degree of the karstic process

that could have deleted potential markers of a littoral environment from the surface, so indicating that the boulders are old. The lack of encrusting and boring fauna did not allow us to carry out C14 dating.

Most boulders have A-axes parallel to the coastline trend, whereas others have their longest axis in an almost E-W direction (Fig. 3a); this is particularly evident for the grouped and embricated boulders that could have struck against obstacles during deposition.

During the field surveys, neither new deposited nor removed megaclasts from the sea waves were observed.

4.2. San Lorenzo area

San Lorenzo is an old farm surrounded by a village located south of the sandy bar that encloses the Pantano Grande and the Pantano Roveto at Vendicari Nature Reserve (Figs. 2c and 4a). Here, the coast is characterized by an articulated gently sloping, rocky platform extending about 400 m in length and 60 m in width, with an average slope of about 8-10%. This is constituted by strongly eroded white-to-yellowish organic calcarenitic and calciruditic deposits of probable Pleistocene age (Lentini *et al.*, 1994). The northern sector of the platform is characterized by a weak slope; southwards, it rises creating a little cliff of about 2-3 m, while further south the platform decreases again (Fig. 4a).

This study area is also characterized by no uplift or a very low one (Ferranti *et al*., 2006; Antonioli *et al*., 2009) as testified by the presence of archaeological remains of a Hellenistic settlement (about 323 B.C. to 30 B.C.) near the Vendicari site. Ponds, dug in the rock for fishing, lie roughly at sea level, indicating that the uplift was of the same order of the sea level rise over the last two thousand years.

The San Lorenzo rocky coast is characterized by erosive littoral features (e.g., pools and potholes) and appears highly fractured. The fractures facilitate the karstic dissolution process and hence the block separation and detachment from the platform; this also accelerates the marine erosion of the platform, with the development of little inlets and the block accumulation at the cliff basis.

In all, 90 boulders have been surveyed (Fig. 4a). They are constituted by calcarenite and are usually rectangular (mainly platy, i.e., with C-axis < 0.6 m); (Fig. 4b), sometimes sub-angular and with sharp broken edges. The boulders have an average volume of about 2.5 m^3 and an estimated weight of about 6.2 t (assuming an average density of 2.3 g/cm^3 based on laboratory analyses). The largest boulder is about 19.6 m^3 (4.2×3.9×1.2 m) with a weight of about 45 t; it lies only 1 m from the coastline, some tens of centimeters above sea level (L52 in Fig. 4a).

Usually, A-axis direction of the largest boulders is almost parallel to the coast trend, but many boulders show an A-axis orientation between N60°E and N120°E (Fig. 4a). This difference could depend on local undulations of the coastline, irregularity of the platform or on the fact that megaclasts can get stuck against each other or against obstacles on the platform. The elongated boulders tend to be imbricated or to have their long axis orthogonal to the direction of the flow.

Most of the mega-blocks do not show fresh biogenic concretions and have few typical marine erosive features but their surface is characterized by alveolar weathering (Figs. 4b and 4c). Therefore, they were probably detached from the platform or carved out from the top of the cliff. Only some blocks show old biogenic concretions and small flat rock pools suggesting that they were removed from the supralittoral zone.

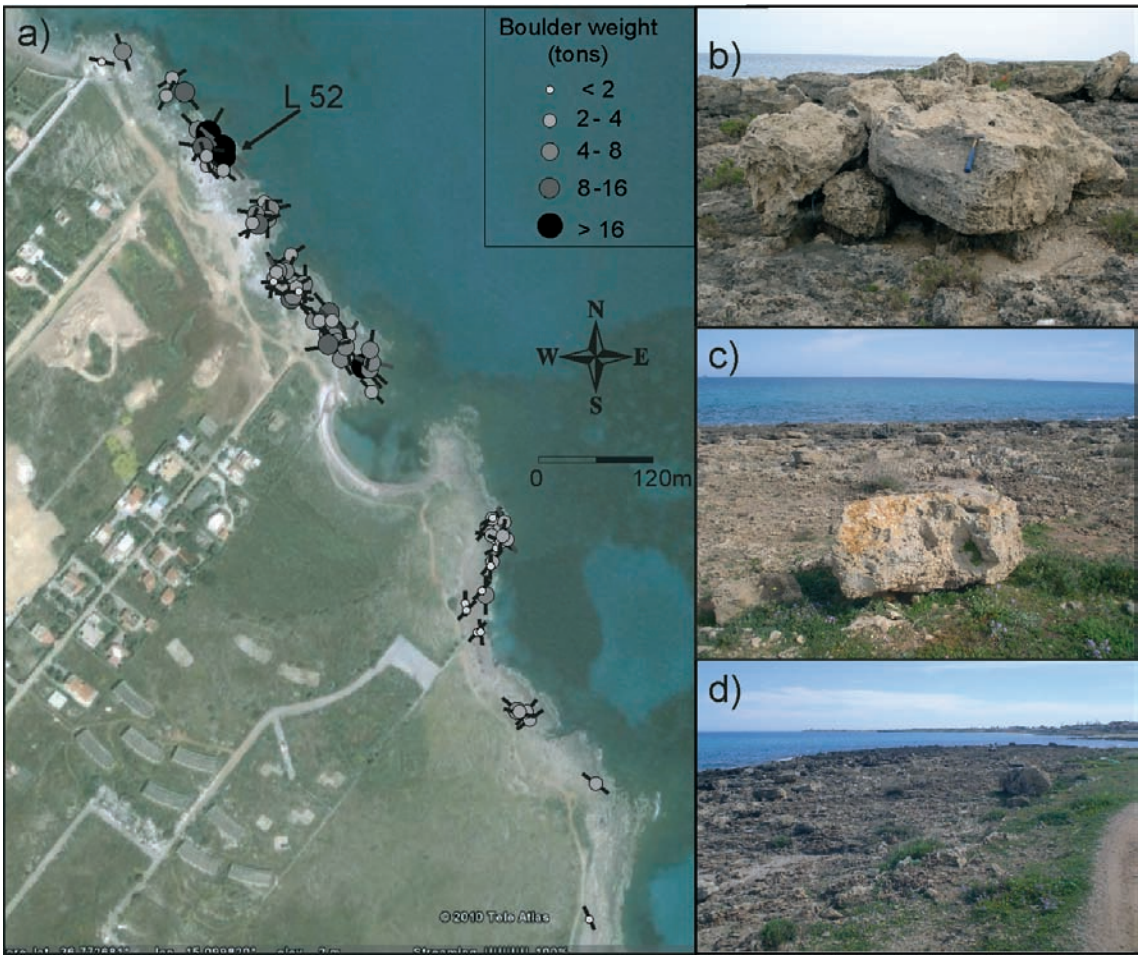

Fig. 4 - Google Earth map showing the boulder location along the San Lorenzo coastland (for location see Fig. 2); dots indicate the different boulder weights and black lines indicate A-axis orientation (a); view of the boulder accumulation in: the northern (b), central (c), and southern areas (d).

During the second and the third field surveys, we observed several new emplaced boulders, most of them near the shoreline and with A-axis < 1 m. In the southernmost area, we also noticed a lot of megaclasts clearly emplaced by storm waves in the tide influence area.

5. Data analysis

5.1. Statistical analysis of the boulders

To understand the cause of boulder emplacement, we performed a statistical analysis of their distribution on the coast, in the studied sites and compared our results with those obtained analyzing the 175 boulders surveyed at Vendicari by Barbano *et al*. (2010).

Although the rocky platforms of the studied areas have about the same width, the boulder-size distributions at the Capo Campolato, San Lorenzo and Vendicari sites are quite different (Figs. 5

and 6). At Capo Campolato, the boulders are placed up to 80 m from the shoreline and there are no boulders in the first 10 m (Fig. 5a); at Vendicari we found boulders up to a 60 m distance (Fig. 5b) whereas at San Lorenzo they stop at 30 m (Fig. 5c). At Capo Campolato (Fig. 5a) and at Vendicari (Fig. 5b), there is no landward fining trend, whereas at the San Lorenzo site it seems that the heaviest boulders stop after a short distance in land (Fig. 5c).

At Vendicari, the frequency distribution of boulders with distance shows that boulders follow three fining trends at different distances from the shoreline (Fig. 5b): indeed, most of the megaclasts stop in the first 20 m, a group stop before 40 m and a small number is found beyond this distance (Fig. 6b), whereas at Capo Campolato there is a concentration of boulders at about 60 m (Fig. 6a) and at San Lorenzo most of the boulders are between 10 and 15 m (Fig. 6c). This behaviour could be related to waves which, depending on their characteristics, are able to transport and emplace the boulders at different distances and probably also to morphological obstacles that can affect boulder movement.

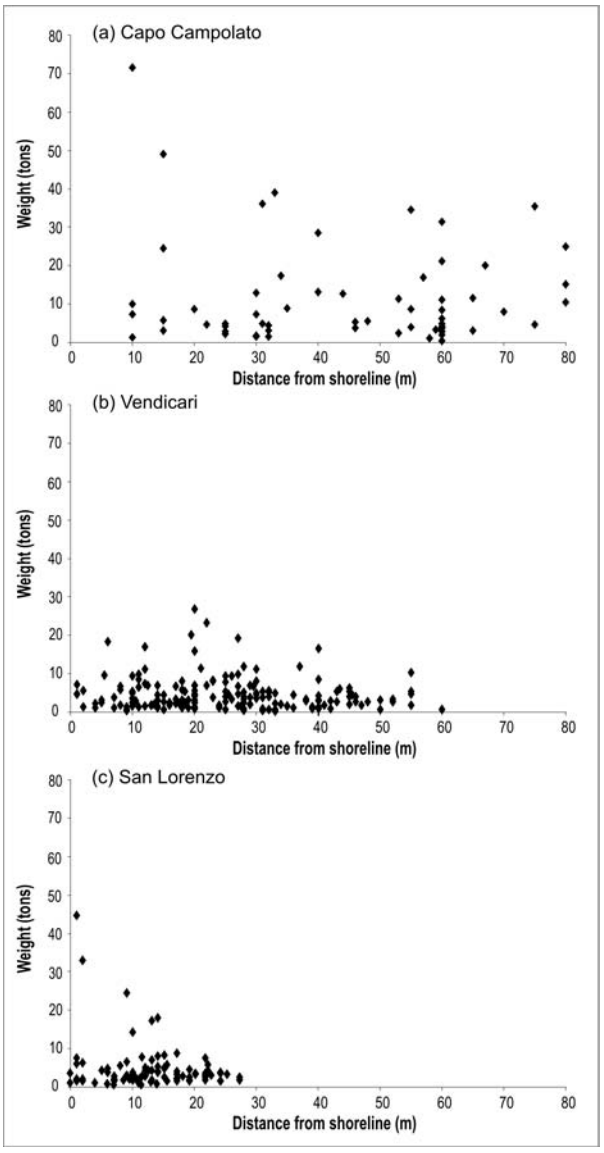

Fig. 5 - Grain size (tons) distribution from the coastal edge for boulders at Capo Campolato (a), at Vendicari (b), and at San Lorenzo (c).

5.2. Boulder-transport equations

Since the boulder shape can be generally ascribed to a parallelepiped, and we observed several boulders leaving continuous tracks on the platform, we hypothesized that the most probable transport mechanisms are of sliding and entraining into the flow, as proposed by Noormets *et al*. (2004); whereas we did not consider the transport by rolling or saltation, because it is typical of well-rounded and ellipsoidal boulders (Goto *et al*., 2007).

Following the Noormets' *et al*. (2004) approach, we first estimated the wave heights at the time the boulders were deposited in their final inland position; then, we assessed the transport

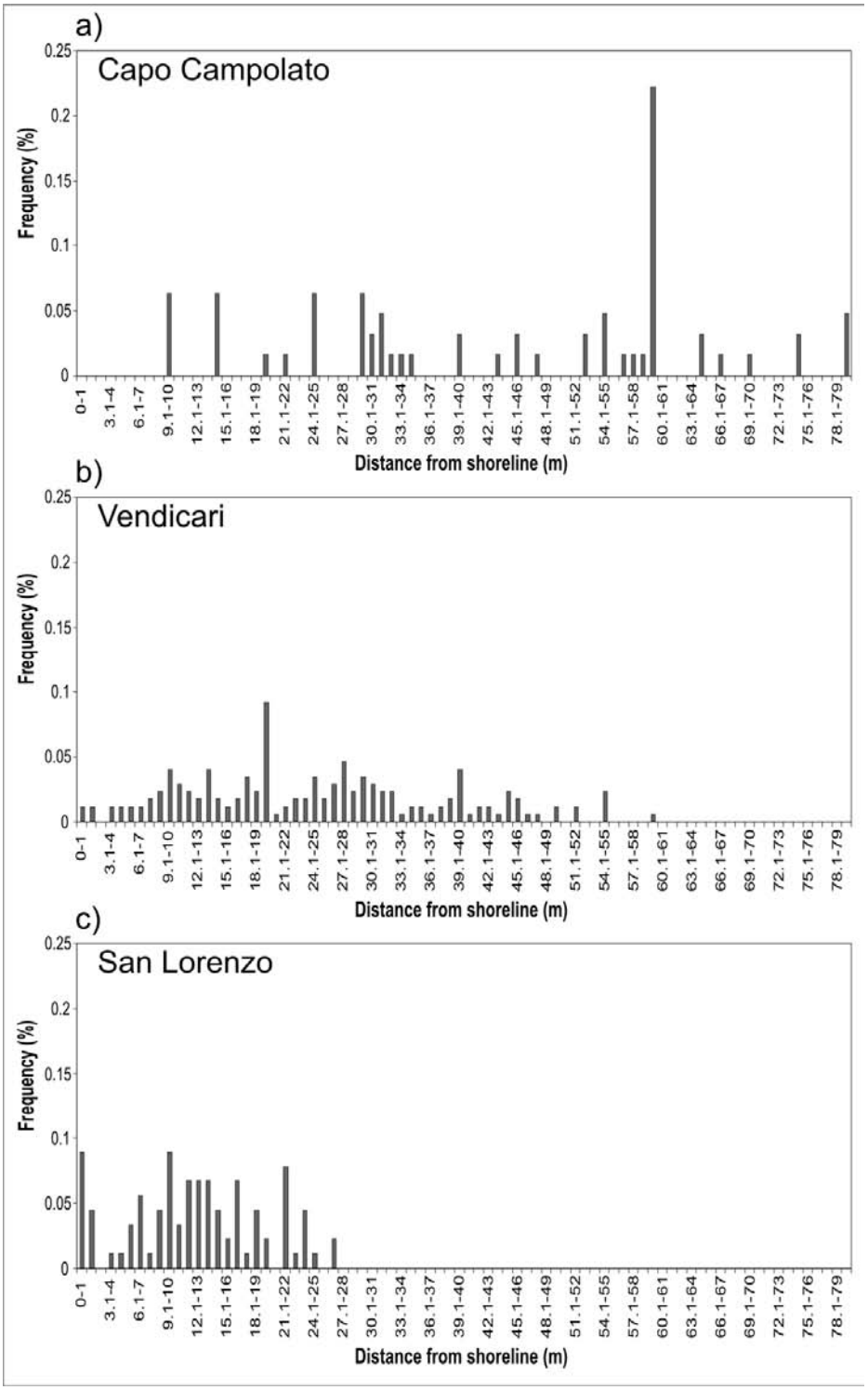

Fig. 6 - Frequency of boulders vs. distance from coastline at Capo Campolato (a), at Vendicari (b), and at San Lorenzo (c).

limit of boulders by the largest known storm waves in the past. Therefore, since boulders deposited beyond this limit are probably transported by waves with a longer period and hence wavelength, such as the tsunamis, we also estimated the transport limit of boulders by the known historical tsunamis (Barbano *et al*., 2010).

In the model that assumes boulders are entrained into the flow [for detail on hydrodynamic calculations see Noormets *et al*. (2004)], we can estimate the wave height of storms (*Hs*) and tsunamis (*Ht*) capable of depositing the boulder in its final position inland from:

$$Hs = [2\ (\rho_s-\rho_w/\rho_w)\ bc] / (C_D\ c + C_L\ b) \quad (1)$$

$$Ht = [0.5\ (\rho_s-\rho_w/\rho_w)\ bc] / (C_D\ c + C_L\ b) \quad (2)$$

where ρ_w is the density of water at 1.02 g/ml, ρ_s is the density of the boulders, C_D is the drag coefficient = 1.95, C_L lift coefficient = 0.178, a is the A-axis of boulder, b the B-axis of boulder, c is the C-axis of boulder.

In the model that assumes boulders move by sliding onto the platform [for details on hydrodynamic calculations see Noormets *et al*. (2004)], the final storm (*Hs*) and tsunami (*Ht*) heights that are equal to the minimum wave height required to move the megaclasts on the platform, will be:

$$Hs = [2\ \mu\ \rho_s\ abc] / (C_D\ \rho_w\ ac) \quad (3)$$

$$Ht = [0.5\ \mu\ \rho_s\ abc] / (C_D\ \rho_w\ ac) \quad (4)$$

where μ is the coefficient of friction = 0.7 (Kabardin, 1990).

Applying Eqs. (1), (2), (3), (4) for both study sites, we calculated the minimum storm and tsunami wave heights at the moment that boulders are emplaced in their inland position (Figs. 7 and 8).

In order to assess if storms were able to emplace a given boulder in its final position, we can compare the computed value of the storm wave height at the final inland distance of the boulder with the flooding landward limit of the strongest storm waves in the study area. The maximum water inundation of strongest storms has been computed using the Cox and Machemehl (1986) and Noormets *et al*. (2004) equations. According to these authors, the decay in height of a wave overriding a shore is proportional to the distance *X* and inversely proportional to wave period *T*:

$$H_i = \left(\sqrt{R-E} - \frac{5X_i}{T\sqrt{g}} \right)^2 \quad (5)$$

where H_i is the wave height at the distance X_i; R is the maximum height of the wave at the breaking point corresponding to H_b of the Sunamura and Horikawa (1974) equation (Table 1); and E is the cliff elevation.

Considering that at the maximum water flooding along a coastal area with slope α ($X_i = X_{max}/\cos\alpha$),

the wave height H_i becomes nil, we can obtain the X_{max} from the Noormets' *et al*. (2004) equation:

$$X_{\max} = \left(T \cdot \sqrt{g} \cdot \sqrt{R - E} \cdot \cos\alpha\right) \Big/ 5 \tag{6}$$

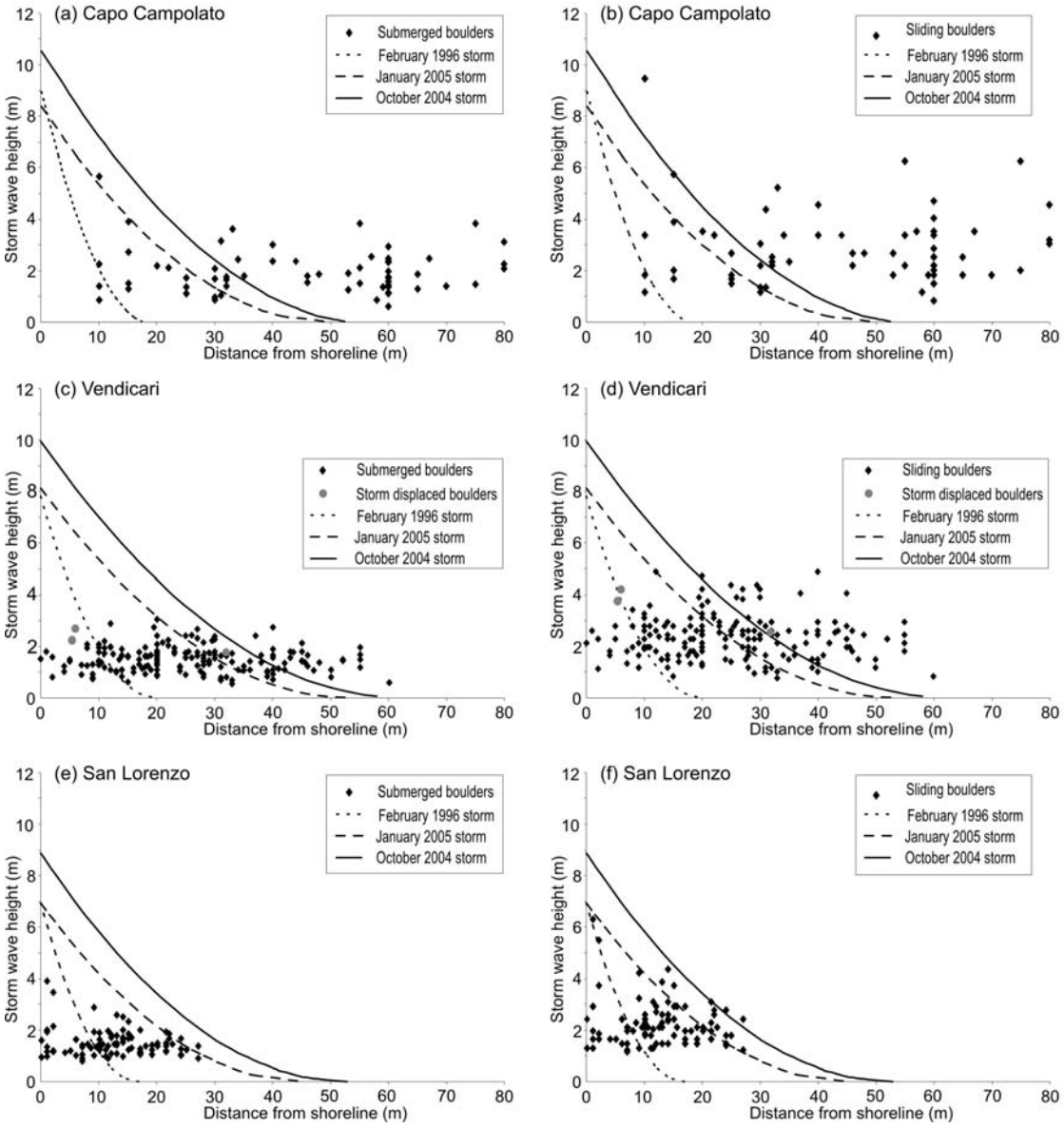

Fig. 7 - Flooding landward limit of the strongest storm waves at: Capo Campolato site [(a) and (b)]; Vendicari site [(c) and (d)]; San Lorenzo site [(e) and (f)]; (storm breaking wave H_b and relative period are reported in Table 1). Black diamonds are the values of the storm wave heights when each boulder was deposited at its distance from the shoreline, computed by applying the flow transport mechanism (graphs on the left) and the sliding transport mechanism (graphs on the right) by Noormets *et al*. (2004). Grey dots are boulders emplaced by the 2009 winter storm waves at Vendicari.

where cos α represents the cathetus of a rectangular triangle, corresponding to the mean slope taken from the sloping overland profile of the typical coast of the study areas.

Fig. 7 shows the wave attenuation with distance for the maximum known storms (Table 1) at Capo Campolato and San Lorenzo, and the ones of Vendicari (from Barbano *et al*., 2010), obtained from Eqs. (5) and (6), where $R = H_b$ and $E = 0$, because the coast usually has no scarp in these areas, compared with the wave heights (*Hs*) computed for each boulder at the transport distance from Eqs. (1) and (3). In truth, the central area of the San Lorenzo site has a 2 m high cliff, but we did not consider it because using $E > 0$ the wave height is reduced by the same value as the cliff and consequently the inland penetration decreases, whereas using $E = 0$ the maximum height and therefore the maximum inland distance is reached.

In order to compare computed tsunami heights *Ht* [Eqs. (2) and (4)] that could have deposited

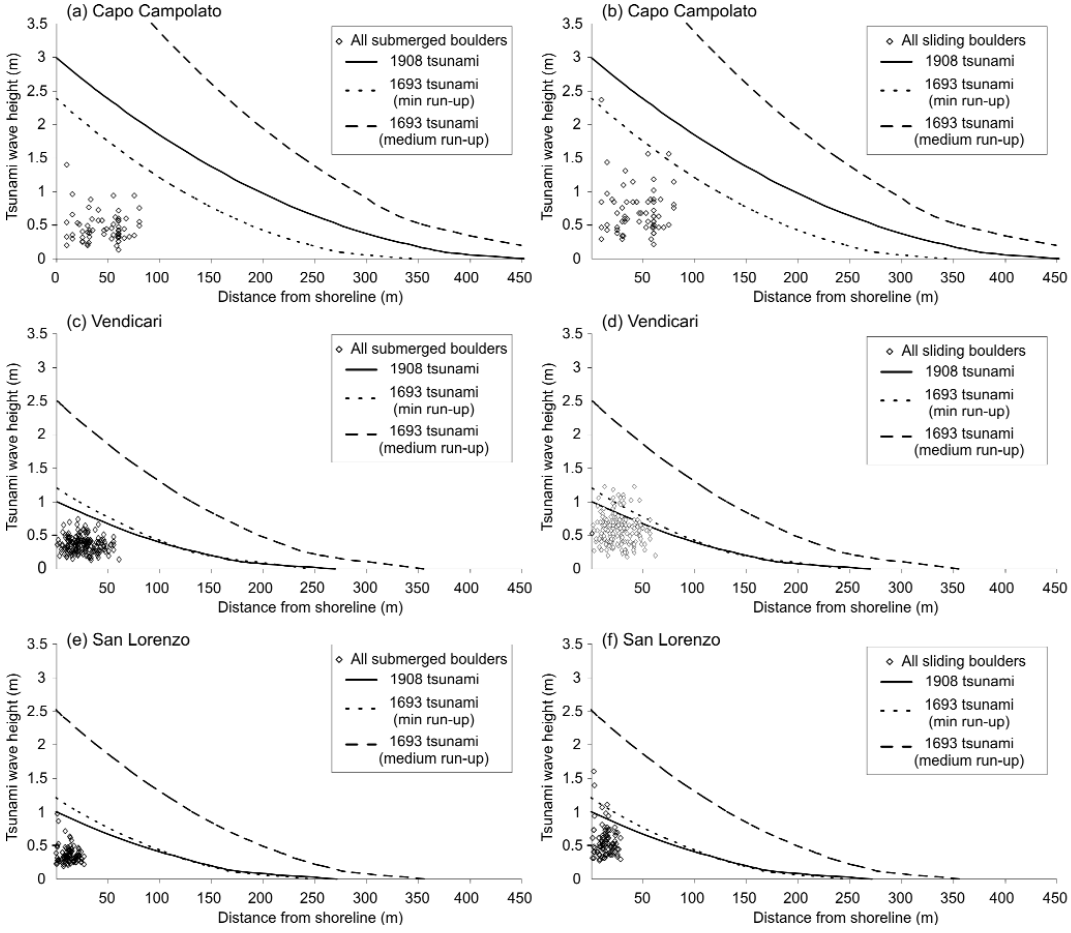

Fig. 8 - Flooding landward limit of three probable tsunamis (1908 tsunami, run-up $R = 1$ m and period $T = 8$ min; 1693 tsunami, $Rmin = 1.2$ m, $Rmed = 2.5$ m and $T = 7$ min) compared with the tsunami heights (*Ht*) the moment that boulders are emplaced in their inland position, computed by applying the flow transport mechanism (left graphs) and the sliding transport mechanism (right graphs) Capo Campolato [(a) and (b)]; Vendicari [(c) and (d)]; San Lorenzo [(e) and (f)].

the boulders in their position with the known historical waves inundating the study area, we estimated the maximum tsunami flooding from Eq. (6), using wave heights and period of historical events (Fig. 8). For Capo Campolato, we used the run-up observed at Augusta for the 1693 tsunami (Fig. 1b) and at Brucoli for the 1908 tsunami (Fig. 1c). For the Vendicari and San Lorenzo areas, there are no observed tsunami data, so we used average run-up values available in the nearest locations of SE Sicily (Gerardi *et al*., 2008) (Figs. 1b and 1c). For the 1693 historical tsunami, we adopted the minimum run-up $Rmin$ = 1.2 m and a medium run-up $Rmed$ = 2.5 m observed at Siracusa, and for the 1908 tsunami the value of 1 m observed at Marzamemi (Fig. 1c). Furthermore, for the 1908 tsunami, we used a medium wave period T = 8 min reported by historical reports (Platania, 1909; Baratta, 1910), whereas for the 1693 tsunami a medium period of about T = 7 min obtained modelling the tsunami source (Tinti *et al*., 2001). The computed flooding landward limits are compared with the tsunami height (Ht) at the moment that boulders are emplaced in their inland position applying the flow transport mechanism [Eq. (2)] and the sliding transport mechanism [Eq. (4)] (Fig. 8).

5. Discussion

The impacting wave type, the quarrying of the boulders from the platform edge can be viewed as a two-step process: dislodgement and emplacement (Noormets *et al*., 2004). Although essentially a continuous process, the set of forces acting upon the block and the mechanisms of their application are different before and after the megaclast detachment. Moreover, many features control wave formation in the near-shore shallow water zone including seafloor topography, tide conditions, shoreline configuration, and openness to major storm surges and such factors are difficult to incorporate into a transport model. However, in order to identify the most likely shoreline-affecting event, it is necessary to adopt a simplified model determining, for each boulder of interest, a preferred transport mechanism, considering its shape and position. In our analysis, considering the high quarrying capacity due to the high pressure exerted by storm waves, joined to the high degree of pre-existing fracturing on the coastal study areas, we assessed that the boulders were already detached and on the platform or in the sublittoral zone. We decided to apply both transport mechanisms proposed by Normeets *et al*. (2004) to all boulders, on the basis of boulder shape and field observations. This approach highlighted different results between the Vendicari, Capo Campolato and San Lorenzo sites.

At Vendicari, we found that storm waves such as those in February 1996, October 2004 and January 2005, were able to deposit boulders of about 6 t up to 30-40 m from the shoreline; this finding was also supported by direct field observations of boulders of about 6 t moved up to 32 m by January 2009 storms (Barbano *et al*., 2010). In this area, the boulder characteristics (fresh algal, and other biogenic encrustations, etc.) show that they were often in sublittoral zones from where they were dragged up. Moreover, they are distributed at different distances from the shoreline, suggesting that some boulders were probably deposited by tsunamis because they are far beyond the possible transport limit of boulders by storm waves (Figs. 7c and 7d).

At Capo Campolato, boulders are scattered randomly along the gently sloping, rocky coast from 10 to 80 m from the shoreline (Figs. 5a and 6a), and most of the boulders (Figs. 7a and 7b) are landward beyond the storm wave transport limit. Furthermore, the boulders have no biogenic

encrustations and appear highly eroded. During the survey after the storms, we did not observe moved boulders, although some boulders are compatible with the flooding landward limit of the strongest storm waves; instead, we observed detritus (bottles, wood, reeds, etc.) on the rocky platform up to about 30-40 m from the shoreline.

At San Lorenzo, boulders show a landward fining trend (Fig. 6c) and all boulders are placed within the flooding limit of the strongest storm waves (Figs. 7e and 7f) for both transport mechanisms, even if the computed storm waves have lower breaking heights and therefore the inundation limits are shorter than the ones at Vendicari. At San Lorenzo, we observed several small-size boulders clearly moved by recent storms placed near the shoreline. Moreover, at San Lorenzo a maximum flooding distance of ordinary storm waves has been measured: at the 2-3 m high cliff, the maximum flooding distance is about 20 m from the shoreline; northwards, where the coast becomes flat and gently sloping, it reaches 30 m, a distance where we found types of grass that does not grow in marine water (Figs. 4b and 4c).

At Vendicari and Capo Campolato, the presence of some boulders beyond the flooding landward limit of the strongest known storm waves, could indicate the action of different waves, that attenuate further inland; this would suggest that these boulders could have been deposited by stronger unknown storm waves or, more probably, by tsunamis having a longer period and therefore a lower attenuation.

The flooding landward limit of three probable waves, such as those of historical tsunamis, shows that nearly all the boulders should be emplaced by a wave of about 1 m like the 1908 tsunami in the flow transport mechanism at Vendicari (Fig. 8c) and San Lorenzo (Fig. 8e), and of about 2.5 m like the 1693 tsunami in the sliding transport mechanism (Figs. 8d and 8f, respectively), whereas at Capo Campolato a minimum wave of 2.5 m is needed to move some boulders (Figs. 8a and 8b).

At the Capo Campolato site, the lack of boulders in the first 10 m of the platform (Fig. 6a) could be explained by its geographic and morphologic position: the site lies at the northern tip of an almost NW-SE trending promontory (Figs. 1a and 2b), so it seems less exposed to the effects of the strongest storms coming from ESE-WNW and SE-NW direction. Moreover, the occurrence of most boulders of probable tsunami origin could be related to the NE-SW geographical exposure, a plausible direction of tsunami flood, and to the vicinity of the tsumamigenic sources (Fig. 1a).

On the contrary, the Vendicari and San Lorenzo sites are located on a roughly NNE-SSW sector of the Sicilian Ionian coast that is intensely subjected to the typical Ionian storms; this could justify the high frequency of boulders in the first 30 m from the shoreline (Figs. 6b and 7c). Furthermore, the lack of boulders farther than 30 m from the coastline at San Lorenzo could be explained by the morphologic features of the area. Indeed, the low-angle, sea-bottom topography, also testified by the small island placed in a north-eastern direction (Fig. 2c), could attenuate the action of north-eastern extreme waves, a direction from which tsunamis arrive. Moreover, in the southernmost coast of Sicily, where Vendicari and San Lorenzo sites are located, tsunami historical data report smaller run-ups with respect to those observed near Capo Campolato (Fig. 1a).

In this study, we verified how the wave length and consequently the wave period, which are the discriminating parameters between storm wave and tsunami, seems to be the factor

controlling the maximum distance of penetration and the potential to transport the boulders inland. Hence, though storm breaking waves can be higher (between 7 and 10 m in the study areas) than tsunamis, they attenuate their energy faster on the coast (X_{max} storm up to 55 m, Fig. 7; X_{max} historical tsunami up to 300 m, Fig. 8).

Although we defined the transport limit of the storm waves and identified the boulders of probable tsunami origin, we cannot exclude that some boulders within the storm transport limits could be deposited by tsunamis, especially in the San Lorenzo area; likewise, it is possible that a series of higher-energy storms than the known ones are responsible for boulder accumulation or that the mechanism of emplacement is different. Imamura *et al*. (2008) showed for instance that a rolling or jumping transport mechanism can move more inland boulders than a sliding mechanism. At the Vendicari site, we dated three samples collected on boulders beyond the transport limit of the storm waves (Barbano *et al*., 2010). Results indicated that the two samples have a very recent age and their deposition would have occurred about two or three centuries ago. Even if only few datings are available at the moment, we can tentatively compare these radiocarbon ages with the historical tsunami catalogue, therefore the deposition of two boulders could be related to the 1908 or 1693 tsunamis. We suggest the 1693 event because its probable source is closer to the study area than the 1908 tsunami source, even if tsunami wave transport models reveal that a wave of about 1 m, like the one reported for the 1908 event in the study area, could have emplaced almost all boulders at Vendicari. Emplacement of the third boulder occurred probably after 650-930 A.D. This inundation could be either an unknown event or one of the historical tsunamis (1169, 1542, 1693) that affected the Ionian coast of Sicily. In fact, since the radiocarbon dating was made on serpulids and on lithophaga shells, the estimate age is the time of organism death, but probably not the moment of the boulder's final displacement.

More radiocarbon datings and absolute age dating of material at the bottom of the boulder, such as optically stimulated luminescence or cosmogenic isotope techniques are necessary to gather a correct imprint of the boulder emplacement in order to correlate them with eventual paleotsunami events, mainly at Capo Campolato where boulders have no biogenic encrustations.

6. Conclusion

We investigated the distribution of the boulders deposited on the south-eastern Sicilian coast in order to verify their origin, i.e., whether storm waves or tsunamis were responsible for their detachment, transport and deposition. Direct field observation of boulders before and after storms showed that some boulders at Vendicari and San Lorenzo were moved, transported, deposited and also removed by storms.

The assessment of the minimum wave height required to transport the boulders inland, following Noormets' *et al*. (2004) approach, compared with the transport limit distance of known storms and tsunamis occurring in the Ionian Sea, showed that both events can displace the boulders. However, because of their size and distance from shoreline, some of them probably have a tsunami origin. In fact, storm waves are not capable of transporting large blocks far onto the platform as a consequence of their rapid dissipation after breaking, so that most blocks stop on the terrace in the first 40 m from the shore. Emplacement of the larger boulders farther from the shore seems to require waves with longer periods than those usually produced by storms in

the Ionian Sea. Since a tsunami wave has a longer period than a storm wave, it is capable of shifting megaclasts farther inland. Based on our analysis, we argue that only tsunamis or unknown extraordinary strong storms can have transported and emplaced these boulders.

Summarising, we showed that strong storms, such as the February 1996, October 2004, and January 2005 events registered in the Ionian Sea, have sufficient energy to move almost all boulders to their present location at the Vendicari and San Lorenzo study areas, but the identification of transport limit of the strong storm waves allowed us to identify many boulders which are displaced far beyond this limit in Vendicari site. At Capo Campolato, most of the boulders lie beyond the flooding limit of the strongest storms; these large boulders, eroded and without biogenic encrustation, mainly scattered between 40 m and 80 m on the platform, probably have a tsunami origin, also considering the geographic exposure of the site, close to tsunami sources like the 1169 and 1693 events.

Acknowledgements. This work was funded by the Italian Civil Protection Department in the frame of the 2007-2009 agreement with the Istituto Nazionale di Geofisica e Vulcanologia - INGV (Seismological Project S1). Many thanks are due to J. Bourgeois, P.M. De Martini, D. Pantosti and A. Smedile for stimulating discussion on boulder accumulation causes. The students F. Bombaci, M.C. Marzullo and M. Raniolo helped us during the boulder surveys. We wish to thank A. Armigliato and G. Mastronuzzi whose suggestions contributed to improve the original manuscript. The present paper was presented at the 28th General Assembly of the "Gruppo Nazionale di Geofisica della Terra Solida", held in Trieste from November 16 to 19, 2009.

REFERENCES

Antonioli F., Ferranti L., Fontana A., Amorosi A.M., Bondesan A., Braitenberg C., Dutton A., Fontolan G., Furlani S., Lambeck K., Mastronuzzi G., Monaco C., Spada G. and Stocchi P.; 2009: *Holocene relative sea-level changes and vertical movements along the Italian and Istrian coastlines*. Quatern. Int., **206**, 102–133.

APAT; 2006: A*tlante delle onde dei mari italiani.* Dip. Tutela Acque Interne e Marine. Servizio Mareografico, Roma, 152 pp.

Baratta M.; 1910: *La catastrofe sismica calabro-messinese (28 dicembre 1908).* Relazione alla Soc. Geogr. Ital., Roma, 426 pp.

Barbano M.S., De Martini P.M., Pantosti D., Smedile A., Del Carlo P., Gerardi F., Guarnieri P. and Pirrotta C.; 2009: *In search of tsunami deposits along the eastern coast of Sicily (Italy): the state of the art.* In: Guarnieri P. (ed), Recent Progress on Earthquake Geology, Nova Science Publishers, pp. 109-146.

Barbano M.S., Pirrotta C. and Gerardi F.; 2010: *Large boulders along the south-eastern Ionian coast of Sicily: storm or tsunami deposits?* Mar. Geol., **275**, 140-154.

Bourgeois J. and MacInnes B.; 2010: *Tsunami boulder transport and other dramatic effects of the 15 November 2006 central Kuril Islands tsunami on the island of Matua*. Z. Geomorphol., **54**, 175–195.

Bourrouilh-Le Jan F.G. and Talandier J.; 1985: *Sedimentation et fracturation de haute energie en milieu recifal: Tsunamis, ouragans et cyclones et leurs effets sur la sedimentologie et la geomorphologie d'un atoll: Motu et hoa, a rangiroa, Tuamotu, Pacifique SE.* Mar. Geol., **67**, 263–333.

Bryant E.A. and Haslett S.K.; 2007: *Catastrophic wave erosion, Bristol Channel, United Kingdom: impact of tsunami?* J. Geol., **115**, 253–269.

Cox J.C. and Machemehl J.; 1986: *Overland bore propagation due to overtopping wave.* J. Waterway, Port, Coastal and Ocean Engineering, **112**, 161–163.

Dawson A.G., Stewart I., Morton R.A., Richmond B.M., Jaffe B.E. and Gelfenbaum G.; 2008: *Reply to Comments by Kelletat (2008) comments to Dawson A.G. and Stewart I.(2007) tsunami deposits in the geological record.*

Sediment. Geol., **211**, 92-93.

De Lange W.P., De Lange P.J. and Moon V.G.; 2006: *Boulder transport by waterspouts: an example from Aorangi Island, New Zealand.* Mar. Geol., **230**, 115–125.

De Martini P.M., Barbano M.S., Smedile A., Gerardi F., Pantosti D., Del Carlo P. and Pirrotta C.; 2010: *A unique 4000 yrs long geological record of multiple tsunami inundations in the Augusta Bay (eastern Sicily, Italy).* Mar. Geol., **276**, 42-57.

Emanuel K.A.; 2005: *Genesis and maintenance of "Mediterranean hurricanes".* Adv. Geosci., **2**, 217–220.

Etienne S. and Paris R.; 2010: *Boulder accumulations related to storms on the south coast of the Reykjanes Peninsula (Iceland).* Geomorphology, **114**, 55–70.

Ferranti L., Antonioli F., Mauz B., Amorosi A., Dai Pra G., Mastronuzzi G., Monaco C., Orru` P., Pappalardo M., Radtke U., Renda P., Romano P., Sansò P. and Verrubbi V.; 2006: *Markers of the last interglacial sea level highstand along the coast of Italy: tectonic implications.* Quatern. Int., **145–146**, 30–54.

Fita L., Romero R., Luque A., Emanuel K. and Ramis C.; 2007: *Analysis of the environments of seven Mediterranean tropical-like storms using an axisymmetric, nonhydrostatic, cloud resolving model.* Nat. Hazards Earth Syst. Sci., **7**, 41–56.

Gerardi F., Barbano M.S., De Martini P.M. and Pantosti D.; 2008: *Discrimination of tsunami sources (earthquake vs. landslide) on the basis of historical data in eastern Sicily and southern Calabria.* Bull. Seism. Soc. Am., **98**, 2795-2805.

Gianfreda F., Miglietta M. and Sansò P.; 2005: *Tornadoes in Southern Apulia (Italy).* Nat. Hazards, **34**, 71–89.

Goff J., Dudley W.C., deMaintenon M.J., Cain G. and Coney J.P.; 2006: *The largest local tsunami in 20th century Hawaii.* Mar. Geol., **226**, 65–79.

Goff J., McFadgen B.G. and Chague-Goff C.; 2004: *Sedimentary differences between the 2002 Easter storm and the 15th-century Okoropunga tsunami, southeastern North Island, New Zealand.* Mar. Geol., **204**, 235–250.

Goto K., Chavanich S.A., Imamura F., Kunthasap P., Matsui T., Minoura K., Sugawara D. and Yanagisawa H.; 2007: *Distribution, origin and transport process of boulders deposited by the 2004 Indian Ocean tsunami at Pakarang Cape, Thailand.* Sediment. Geol., **202**, 821–837.

Goto K., Miyagi K., Kawamata H. and Imamura F.; 2010: *Discrimination of boulders deposited by tsunamis and storm waves at Ishigaki Island, Japan.* Mar. Geol., **269**, 34–45.

Goto K., Okada K. and Imamura F.; 2009: *Characteristics and hydrodynamics of boulders transported by storm wave at Kudaka Island, Japan.* Mar. Geol., **262**, 14–24.

Guidoboni E., Comastri A. and Traina G.; 1994: *Catalogue of earthquakes and tsunamis in the Mediterranean area up to 10th century.* Ist. Naz. di Geofis. e Vulcanol., Rome, 504 pp.

Hall A.M., Hansom J.D., Williams D.M. and Jarvis J.; 2006: *Distribution, geomorphology and lithofacies of cliff-top storm deposits: examples from the high-energy coasts of Scotland and Ireland.* Mar. Geol., **232**, 131–155.

Hansom J.D. and Hall A.M.; 2009: *Magnitude and frequency of extra-tropical North Atlantic cyclones: A chronology from cliff-top storm deposits.* Quatern. Int., **195**, 42–52.

Hansom J.D., Barltrop N.D.P. and Hall A.M.; 2008: *Modelling the processes of cliff-top erosion and deposition under extreme storm waves.* Mar. Geol., **253**, 36–50.

Hills J.G. and Mader C.L.; 1997: *Tsunami produced by the impact of small asteroids.* Ann. NY Acad. Sci., **882**, 381-394.

Imamura F., Goto K. and Ohkubo S.; 2008: *A numerical model for the transport of a boulder by tsunami.* J. Geophys. Res., **113**, C01008, DOI 10.1029/2007JC004170.

Istituto Idrografico della Marina; 1999: *Carta Nautica da Capo Passero a Capo S. Croce, scala 1:100.000.*

Kabardin O.; 1990: *Koolifüüsika käsiraamat.* Valgus, Tallinn., 320 pp.

Kelletat D.; 2008: *Comments to Dawson, A.G. and Stewart, I. (2007), Tsunami deposits in the geological record (Sedimentary Geology 200, 166-183).* Sediment. Geol., **211**, 87-91.

Kelletat D. and Schellmann G.; 2002: *Tsunami on Cyprus: field evidences and 14C dating results.* Z. Geomorphol., **46**, 19–34.

Kelletat D., Scheffers A. and Scheffers S.; 2004: *Holocene tsunami deposits on the Bahaman Islands of Long Island*

and Eleuthera. Z. Geomorphol., **48**, 519–540.

Kortekaas S. and Dawson A.G.; 2007: *Distinguishing between tsunami and storm deposits: an example from Martinhal, SW Portugal.* Sediment. Geol., **200**, 208–221.

Lentini F., Carbone S. and Catalano S.; 1994: *Main structural domains of the central Mediterranean region and their Neogene tectonic evolution.* Boll. Geof. Teor. Appl., **36**, 103–125.

Lionello P., Malanotte-Rizzoli P. and Boscolo R.; 2006: *Mediterranean climate variability.* In: Developments in Earth and Environmental Sciences, Elsevier, 438 pp.

Lorito S., Tiberti M.M., Basili R., Piatanesi A. and Valensise G.; 2008: *Earthquake-generated tsunamis in the Mediterranean Sea: scenarios of potential threats to Southern Italy.* J. Geophys. Res., **113**, B01301, DOI 10.1029/2007JB004943.

Maouche S., Morhange C. and Meghraoui M.; 2009: *Large boulder accumulation on the Algerian coast evidence tsunami events in the western Mediterranean.* Mar. Geol., **262**, 96–104.

Mastronuzzi G. and Sansò P.; 2000: *Boulders transport by catastrophic waves along the Ionian coast of Apulia (Southern Italy).* Mar. Geol., **170**, 93-103.

Mastronuzzi G. and Sansò P.; 2004: *Large boulder accumulations by extreme waves along the Adriatic coast of southern Apulia (Italy).* Quatern. Int., **120**, 173–184.

Mastronuzzi G., Pignatelli C., Sansò P. and Selleri G.; 2007: *Boulder accumulations produced by the 20th February 1743 tsunami along the coast of southeastern Salento (Apulia region, Italy)*. Mar. Geol., **242**, 191-205.

Monserrat S., Vilibiç I. and Rabinovich A.B.; 2006: *Meteotsunamis: atmospherically induced destructive ocean waves in the tsunami frequency band.* Nat. Hazard Earth Syst. Sci., **6**, 1035–1051.

Morton R.A., Gelfenbaum G. and Jaffe B.E.; 2007: *Physical criteria for distinguishing sandy tsunami and storm deposits using modern examples*. Sediment. Geol., **200**, 184–207.

Morton R.A., Richmond B.M., Jaffe B.E. and Gelfenbaum G.; 2006: *Reconnaissance investigation of Caribbean extreme wave deposits - Preliminary observations, interpretations, and research direction.* Open File Report 1293, USGS., 46 pp.

Morton R.A., Richmond B.M., Jaffe B.E. and Gelfenbaum G.; 2008: *Coarse-clast ridge complexes of the Caribbean: a preliminary basis for distinguishing tsunami and storm-wave origins.* J. Sediment. Res., **78,** 624–637.

Nanayama F., Shigeno K., Satake K., Shimokawa K., Koitabashi S., Mayasaka S. and Ishi M.; 2000: *Sedimentary differences between 1993 Hokkaido-Nansei-Oki tsunami and 1959 Miyakijima typhoon at Tasai, southwestern Hokkaido, northern Japan*. Sediment. Geol., **135**, 255–264.

Noormets R., Crook K.A.W. and Felton E.A.; 2004: *Sedimentology of rocky shorelines: 3. Hydrodynamics of megaclast emplacement and transport on a shore platform, Oahu, Hawaii.* Sediment. Geol., **172**, 41–65.

Noormets R., Felton E.A. and Crook K.A.W.; 2002: *Sedimentology of rocky shorelines: 2. Shoreline megaclasts on the north shore of Oahu, Hawaii- origins and history*. Sediment. Geol., **150**, 31-45.

Nott J.; 1997: *Extremely high-energy wave deposits inside the Great Barrier Reef, Australia: determining the cause-tsunami or tropical cyclone.* Mar. Geol., **141**, 193–207.

Nott J.; 2003: *Tsunami or storm waves?- Determining the origin of a spectacular field of wave emplaced boulders using numerical storm surge and wave models and hydrodynamic transport equations.* J. Coast. Res., **19**, 348–356.

Paris R., Fournier J., Poizot E., Etienne S., Morin J., Lavigne F. and Wassmer P.; 2010: *Boulder and fine sediment transport and deposition by the 2004 tsunami in Lhok Nga (western Banda Aceh, Sumatra, Indonesia): a coupled offshore–onshore model.* Mar. Geol., **268**, 43–54.

Paris R., Wassmer P., Sartohadi J., Lavigne F., Barthomeuf B., Desgages E., Grancher D., Baumert P., Vautier F., Brunstein D. and Gomez C.; 2009: *Tsunamis as geomorphic crises: lessons from the December 26, 2004 tsunami in Lhok Nga, West Banda Aceh (Sumatra, Indonesia).* Geomorphology, **104**, 59–72.

Pignatelli C., Sansò P. and Mastronuzzi G.; 2009: *Evaluation of tsunami flooding using geomorphological evidence.* Mar. Geol., **260**, 6–18.

Platania G.; 1909: *Il maremoto dello stretto di Messina del 28 Dicembre 1908.* Boll. Soc. Sism. Ital., **13**, 369–458.

Pytharoulis I., Craig G.C. and Ballard S.P.; 2000: *The hurricane-like Mediterranean cyclone of January 1995.* Meteorol. Appl., **7**, 261-279.

Sarpkaya T. and Isaacson M.; 1981: *Mechanics of wave forces on offshore structures.* Van Nostrand Reinhold Company

Inc., New York, 650 pp.

Scheffers A.; 2004: *Tsunami imprints on the Leeward Netherlands Antilles (Aruba, Curaçao and Bonaire) and their relation to other coastal problems*. Quatern. Int., **120**, 163–172.

Scheffers A. and Kelletat D.; 2006: *New evidence and datings of Holocene paleo-tsunami events in the Caribbean (Barbados, St. Martin and Anguilla).* In: Mercado-Irizarry A. and Liu P. (eds), Caribbean tsunami hazard, World Scientific, Singapore, pp. 178-202.

Scheffers A. and Scheffers S.; 2006: *Documentation of the impact of hurricane Ivan on the coastline of Bonaire (Netherlands Antilles).* J. Coastal Res., **22**, 1437–1450.

Scheffers A. and Scheffers S.; 2007: *Tsunami deposits on the coastline of west Crete (Greece).* Earth Planet. Sci. Lett., **259**, 613–624.

Scheffers S.R., Scheffers A., Kelletat D. and Bryant E.A.; 2008: *The Holocene paleo-tsunami history of West Australia.* Earth Planet. Sci. Lett., **270**, 137–146.

Scicchitano G., Monaco C. and Tortorici L.; 2007: *Large boulder deposits by tsunami waves along the Ionian coast of south-eastern Sicily (Italy).* Mar. Geol., **238**, 75-91.

Seymour R.J.; 1977: *Estimating wave generation on restricted fetches.* J. Waterway Port C. Dc. Div., Proc. ASCE paper, 12924, **103**, 251-264.

Sunamura T. and Horikawa K.; 1974: T*wo dimensional beach transformation due to waves.* In: Proceedings 14th Coastal Engineering Conference, Am. Soc. Civilian Engineers, pp. 920–938.

Switzer A.D. and Burston J.M.; 2010: *Competing mechanisms for boulder deposition on the southeast Australian coast.* Geomorphology, **114**, 42–54.

Tinti S., Armigliato A. and Bortolucci E.; 2001: *Contribution of tsunami data analysis to constrain the seismic source: the case of the 1693 eastern Sicily earthquake.* J. Seismol., **5**, 41–61.

Tinti S., Armigliato A., Pagnoni G. and Zaniboni F.; 2005: *Scenarios of giant tsunamis of tectonic origin in the Mediterranean.* ISET J. of Earthquake Technology, **42**, 171-188.

Tinti S., Maramai A. and Graziani L.; 2007: *The Italian Tsunami Catalogue (ITC), Version 2.* http://www.ingv.it/servizi-e-risorse/BD/catalogo-tsunami/catalogo-degli-tsunami-italiani.

Vincent C.L.; 1984: *Deepwater wind wave growth with fetch and duration.* Technical Reports num. CERCMP8413, Coastal Engineering Research Center, Vicksburg Ms, 35 pp.

Whelan F. and Kelletat D.; 2005: *Boulder deposits on the southern Spanish Atlantic coast: possible evidence for the 1755 AD Lisbon tsunami.* Sci. Tsunami Haz., **23**, 25-38.

Working group CPTI; 2004: *Catalogo Parametrico dei Terremoti Italiani, version 2004 (CPTI04).* INGV, Bologna. http://emidius.mi.ingv.it/CPTI/.

Corresponding author: Maria Serafina Barbano
Dipartimento di Scienze Geologiche, Università di Catania
Corso Italia 55, 95129 Catania, Italy
Phone: +39 095 7195729; fax: +39 095 7195712; e-mail: barbano@unict.it